Histol Histopathol (2024) 39: 525-531

Histology and Histopathology
From Cell Biology to Tissue Engineering

ORIGINAL ARTICLE Open Access

Differences in neuromuscular junctions between intrinsic muscles of the forepaw and biceps muscles in rats

Jing Qiao[1], Jing-Yu Gu[2] and Bo Li[3]

[1]Department of Plastic Surgery, Huashan Hospital Affiliated to Fudan University, [2]Department of Neurology, Seventh People's Hospital of Shanghai University of Traditional Chinese Medicine and [3]Department of Orthopedic Surgery, Yangpu Hospital, School of Medicine, Tongji University, Shanghai, China

Jing Qiao and Jing-Yu Gu are the first co-authors

Summary. Motor endplates of the interossei muscles become destabilized, whereas those of the biceps muscles remain stable in a rat model of obstetric brachial plexus palsy. However, it is unclear whether the morphology of the motor endplates of the interossei muscles is different from that of the biceps muscles in normal rat. We hypothesized that the motor endplates in the interossei muscles have specific characteristics different from those in the biceps muscles. The motor endplates were labeled with α-bungarotoxin and synaptophysin. The cross-sectional areas of the muscle fibers, the morphologies of the motor endplates, and the absolute and normalized areas (corrected by muscle fiber diameter) of the motor endplates of the interossei muscles and the biceps muscles were compared in rats at 1, 3, and 5 weeks after birth. The cross-sectional area of the interossei muscles and biceps muscle fibers were found to have increased gradually at 1, 3, and 5 weeks, but that of the biceps muscles was larger than that of the interossei muscles. The motor endplates of the interossei muscles and the biceps muscles gradually develop from crescent to pretzel shape after birth, and those of the interossei muscles have a smaller area. At 1, 3, and 5 weeks postnatally, the area of postnatal normalized motor endplates of the interossei muscles was much smaller than that of the biceps muscles. A better understanding of the morphological differences of the motor endplates between the interossei muscles and the biceps muscles may help to understand their physiological and pathological changes.

Key words: Intrinsic hand muscles, Interossei muscles, Biceps muscles, Motor endplate, Rats

Corresponding Author: Bo Li, Department of Orthopedic Surgery, Yangpu Hospital, School of Medicine, Tongji University, Shanghai, China. e-mail: ttpsj@163.com

www.hh.um.es. DOI: 10.14670/HH-18-667

Introduction

Damage to peripheral nerves leads to the degeneration of nerve fibers and the denervation of innervated muscles. Obstetric brachial plexus palsy (OBPP) is typically a traction type injury during childbirth, causing paralysis and contractures of the upper limbs (Lin and Samora, 2022). For OBPP, reconstruction of the intrinsic muscles of the hand (IMH) innervated by the C8-T1 nerves should be done at most within 3 months after birth, while functional improvement for the upper arm muscles innervated by the C5-6 nerves can still be achieved through grafting even up to 30 months later (Boome and Kaye, 1988). The nerve reconstruction of the lower trunk should not exceed 6 months after birth; otherwise, the function of the interossei muscles cannot be improved (Chuang et al., 2005). A rat model of OBPP was simulated, in which the brachial plexus was repaired. It was found that intrinsic muscles of the forepaw (IMF) with denervation are more susceptible to irreversible atrophy than biceps muscles with denervation, and that C8-T1 nerves have a narrower time window for repair compared to C5-6 nerves. This difference is due to the characteristics of the muscle itself (Wu et al., 2013). The OBPP rat model without nerve reconstruction was used for further study. It was shown that there is a difference between denervated IMF and denervated biceps muscles, with IMF undergoing irreversible atrophy and biceps muscles undergoing reversible atrophy. Further studies using a rat model of OBPP that does not involve nerve reconstruction revealed that denervated IMFs and

Abbreviations. OBPP, Obstetric brachial plexus palsy; IMH, intrinsic muscles of the hand; IMF, intrinsic muscles of the forepaw; AChRs, nicotinic acetylcholine receptors; SD, Sprague-Dawley; PFA, paraformaldehyde; PBS, phosphate buffer solution; HE, hematoxylin and eosin.

©The Author(s) 2024. **Open Access.** This article is licensed under a Creative Commons CC-BY International License.

denervated biceps muscles express unique miRNA profiles (Pan et al., 2015) and mRNA profiles (Wu et al., 2016), and that the denervated IMF has no capacity to self-repair, in contrast to the denervated biceps muscles (Wu et al., 2016), and that 5 weeks after denervation, the IMF motor endplate has become unstable, whereas the biceps muscle motor endplate has remained relatively stable. In addition, the denervation-induced deterioration of the motor endplate in the IMF is more severe compared to that of the biceps muscles (Li et al., 2020). Therefore, there might be a difference in motor endplate self-regulation between denervated interossei muscles and denervated biceps muscles, resulting in irreversible atrophy earlier than denervated biceps muscles.

Muscle activity is induced by nerve impulses from motor neuron axons. Motor endplates, serving as chemical synapse that establish connections between motor neurons and skeletal muscle fibers, facilitate the transmission of signals from the terminations of motor neurons to the postsynaptic membrane of muscle fibers. Peripheral nervous system axons consist mainly of five components: terminal Schwann cells, motor nerve endings, synaptic space, postsynaptic membrane, and muscle substance that provides structural support for the postsynaptic membrane. Postsynaptic components include nicotinic acetylcholine receptors (AChRs), which receive acetylcholine released by motor neurons (Mukund and Subramaniam, 2020). Each mature skeletal muscle contains a specific motor endplate to maintain its function.

There are important functional and structural differences between cranial muscles and the quadriceps femoris (Pfister and Zenker, 1984). Cranial muscles have a higher proportion of motor endplate area than limb muscles. In addition, internal laryngeal muscles are less affected by muscle degenerative diseases (Marques et al., 2007; Thomas et al., 2008). Considering that motor endplates have an intricate fine structure that is closely related to their function, so their specific shape may affect the function of the interossei muscles. However, this difference may also make the denervated interossei muscles undergo irreversible atrophy sooner. Currently, most studies focus on the interossei muscles themselves, but few studies focus on the motor endplates of the interossei muscles. Our study focused on the differences in the motor endplates between the interossei muscles and the biceps muscles. We hypothesized that the shape and area of the motor endplates of the interossei muscles are different from that of the biceps muscles.

Materials and methods

Animals and tissue preparation

The study was conducted with eighteen Sprague–Dawley (SD) rats weighing 11-13g. Each rat was exposed to 12 hours of light/dark and provided with food and water as needed. The procedures were conducted according to the guidelines of the National Institutes of Health for the care and use of laboratory animals. Anesthetized intraperitoneally with 1% pentobarbital sodium (0.5 mL/100 g), the rats were perfused transcranially with 0.1 M solution of 4% paraformaldehyde (PFA) in 0.1 M phosphate buffer solution (PBS). Each animal's bilateral interossei muscles and biceps muscles were collected under an operating microscope (Leica, Germany) at 1, 3, and 5 postnatal weeks (six rats at each time point). All of the collected muscles were fixed with 4% PFA at 4°C for 12 hours. The study protocol was ratified by the Committee on Medical Ethics of Yangpu Hospital, Tongji University (Shanghai, China).

Hematoxylin-eosin staining of muscle fibers

To measure the muscle fiber diameters, the interossei muscles and the biceps muscles were stained with hematoxylin and eosin (HE) in line with routine procedures.

Photographs were taken of three sections of a given muscle. Each section was imaged at x200 from microscopic fields at four quadrants. The fiber diameter and the cross-sectional area of muscle fiber in the photographed images was measured by an image processing program (ImageJ V. 1.45s; NIH, Bethesda, MD, USA). Measurements of fiber diameter and the cross-sectional area of muscle fiber were performed on at least 100 selected muscle fibers according to a previously described procedure (Kim et al., 2007). During the analysis, muscle fibers that were partially engaged within the picture frame (edged particles) were automatically excluded. The output image displayed the outlined, numbered, and displayed fibers and structures analyzed.

Histological analysis of motor endplates

The interossei muscles and the biceps muscles were fixed in 4% PFA for 12 hours at 4°C, dehydrated in 30% sucrose for 12 hours, and embedded in the optimal cutting temperature compound. A microtome (Leica, Wetzlar, Germany) was used to slice each muscle longitudinally, and ten sections (20-mm thick) were harvested for morphological analysis. The sections were permeabilized for 30 minutes with 0.3% Triton X-100 in PBS, then blocked for 1 hour at room temperature with 3% bovine serum albumin in PBS; then, overnight at 4°C, they were incubated with primary antibodies targeting synaptophysin (1:50, Abcam, ab8059, Cambridge, MA, USA) and neurofilament heavy chain (1:1000, Abcam, ab8135, Cambridge, MA, USA), respectively. The sections were then incubated for 2 hours with the following second antibodies at 4°C: donkey anti-mouse IgG H&L (Alexa Fluor® 647) (1:200, Ab150107, Cambridge, MA, USA) for synaptophysin, α-Bungarotoxin-ATTO-488 (1:100,

ALO-B-100-AG-0.1, Alomone, Jerusalem, Israel) for AChRs, and donkey anti-rabbit IgG H&L (Alexa Fluor® 647) (1:200, Ab150075, Cambridge, MA, USA) for neurofilament heavy chain. Finally, antifade reagents were then used to mount the sections on slides.

Motor endplate images were acquired using a Leica TCS SP8 confocal microscope (Leica, Solms, Germany) equipped with a 1.4x numerical aperture and 40x objective lens as a series of optical sections separated by 1-μm increments. The record was obtained regardless of how the motor endplates were oriented with respect to the microscope focus plate. A total of 120 motor endplates were obtained from each muscle.

Motor endplate areas and muscle fiber diameters were measured using ImageJ software (ImageJ V. 1.45s; NIH, Bethesda, MD, USA). For each muscle, the normalized endplate area was calculated by dividing the motor endplate's area by the diameter of the muscle fiber (Pan et al., 2016). Measurements were conducted by one blinded investigator after the measurement methods were developed.

Statistical analysis

The images were analyzed by an investigator blinded to the muscle groups. Each value was expressed as the mean ± standard deviation. Post-hoc analysis was performed using a t test with Bonferroni adjustment. Significance was measured at $P<0.05$.

Results

Muscle mass and cross-sectional area of muscle fibers

HE staining showed that the muscle fibers of the normal interossei muscles and the biceps muscles in SD rats at 1, 3, and 5 weeks after birth were arranged neatly. Additionally, the structure of muscle fibers was complete, the cytoplasm was rich and uniform, and the texture was clear (Fig. 1). The cross-sectional area of normal interossei muscles and biceps muscles increased gradually at 1, 3, and 5 weeks, but the cross-sectional area of the biceps muscles was larger than that of the interossei muscles at the same time point (Table 1).

Morphology of postsynaptic motor endplates in the interossei muscles and the biceps muscles

AChR immunofluorescence staining of the interossei muscles and biceps muscles revealed representative images of motor endplates at 1, 3, and 5 weeks postnatally. Normally, motor endplates were located in the center of the muscle fibers of the interossei muscles and the biceps muscles and the motor nerve endings, with neurofilament labeling, were localized around them. The appearance of the motor endplates of the interossei muscles at 1 week was as a crescent moon, while that of the biceps muscles was a plaque (Fig. 2A1-A3, B1-B3). The postsynaptic motor endplates of the

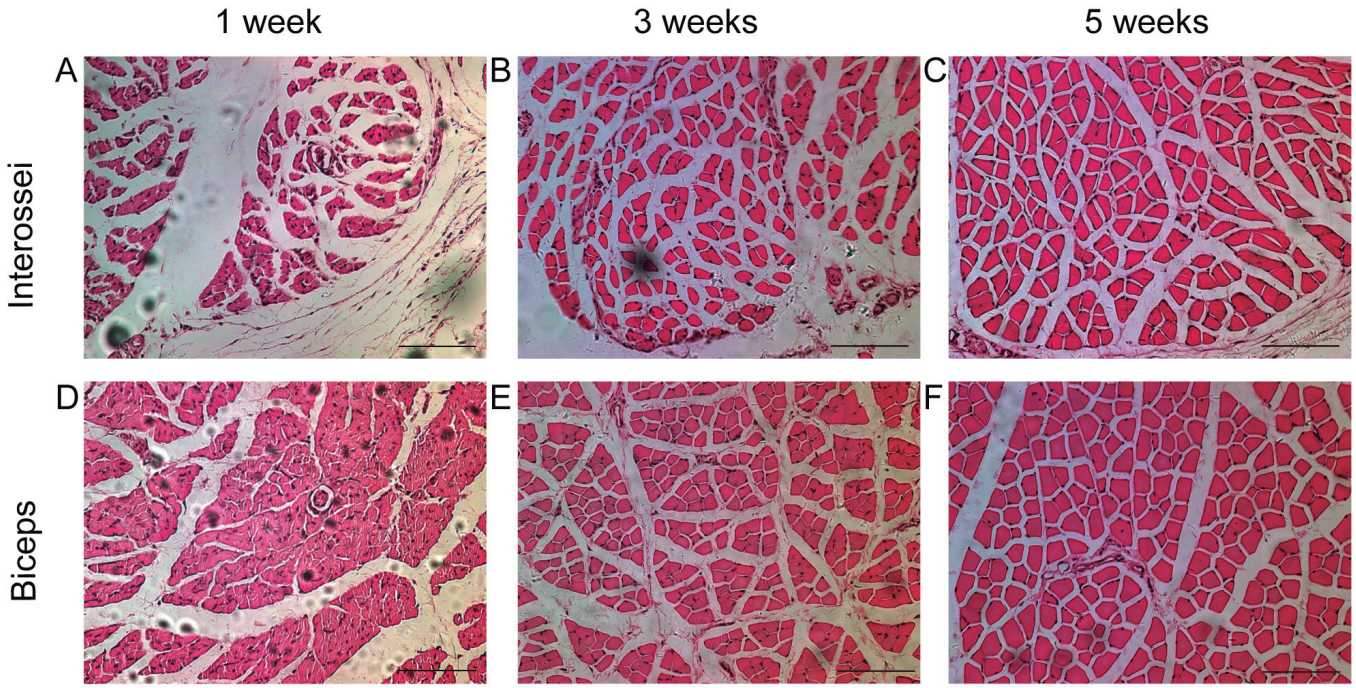

Fig. 1. Histological assessment of the muscle fibers of Sprague-Dawley rats at 1, 3, and 5 postnatal weeks by HE-based staining. **A-C.** HE staining of the interossei muscles at 1, 3, and 5 postnatal weeks. **D-F.** HE staining of the biceps muscles at 1, 3, and 5 postnatal weeks. The muscle fibers of the interossei muscles and the biceps muscles at 1, 3, and 5 weeks postnatally were arranged neatly; the structure of muscle cells was complete; the cytoplasm was rich and uniform; and the texture was clear. Scale bar: 200 μm.

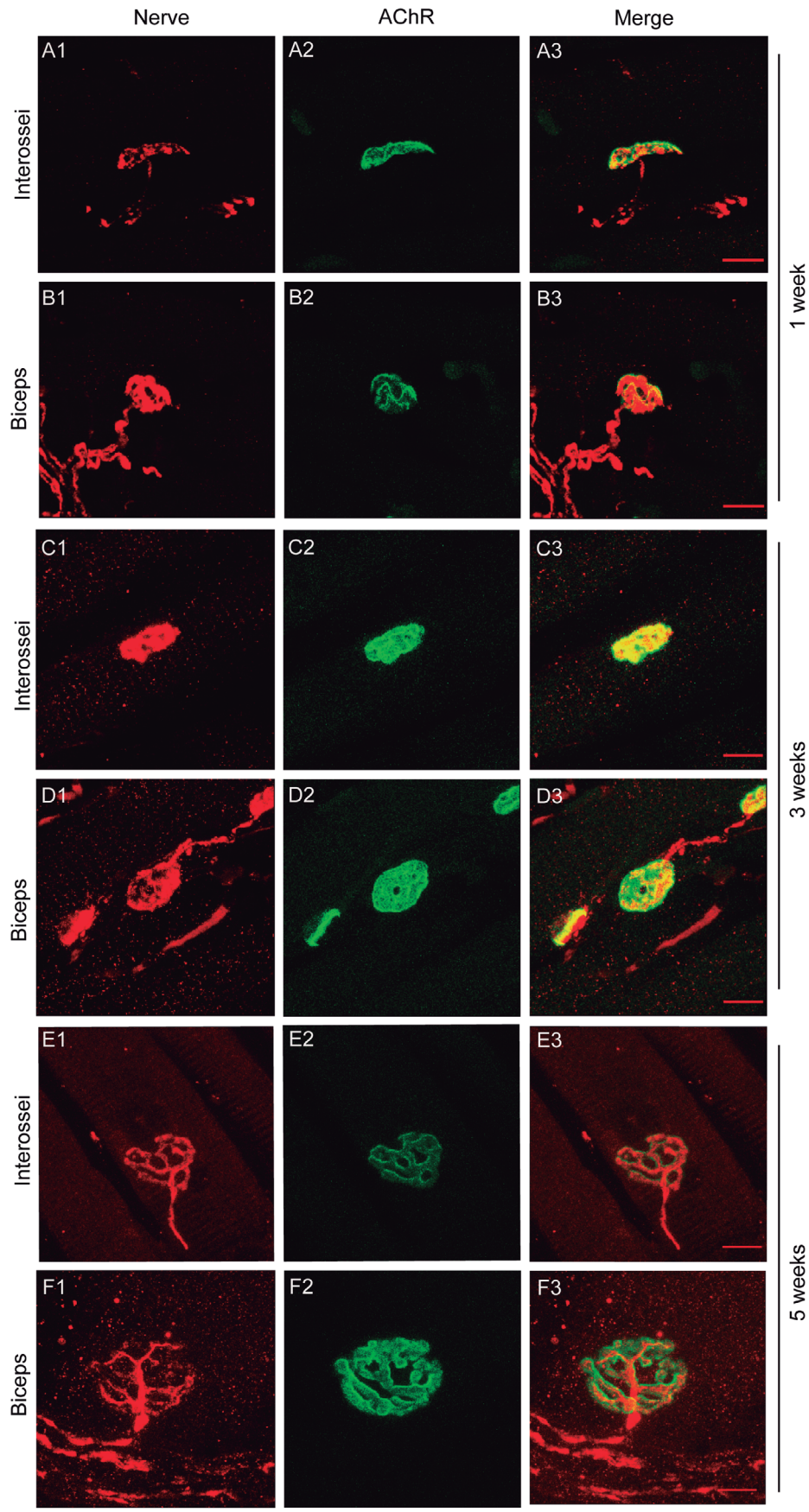

Fig. 2. Representative confocal images of the motor endplate of the interossei muscles and the biceps muscles at 1, 3, and 5 postnatal weeks. The appearance of the motor endplates of the interossei muscles **(A1-A3)** was like a crescent moon, while that of the biceps muscles **(B1-B3)** was a plaque at 1 week postnatally. The postsynaptic motor endplates of the interossei muscles **(C1-C3)** and the biceps muscles **(D1-D3)** were all elliptical at 3 weeks postnatally, but those of the biceps muscles was larger than those of the interossei muscles. The motor endplates of the interossei muscles **(E1-E3)** and the biceps muscles **(F1-F3)** at 5 weeks postnatally were pretzel-shaped, but those of the biceps muscles were larger. Red: Neurofilament; green: motor endplates. Scale bar: 10 μm.

interossei muscles and the biceps muscles at 3 weeks were all elliptical, but those of the biceps muscles were larger than those of the interossei muscles (Fig. 2 C1-C3, D1-D3). The postsynaptic motor endplates of the interossei muscles and the biceps muscles at 5 weeks showed the classical appearance of motor endplates, sometimes referred to as pretzel-shaped, but those of the biceps muscles were larger (Fig. 2E1-E3, F1-F3). Table 1 lists the resulting measurements of normalized motor endplates. The area of normalized motor endplates in the interossei muscles was (6.9±1.1), (7.6±0.9), and (9.1±1.1) (μm^2), while that in the biceps muscles was (8.0±0.9), (11.9±1.7), and (13.4±1.0) (μm^2) at 1, 3, and 5 weeks postnatal, respectively. The area of postnatal normalized motor endplates of the interossei muscles was much smaller than that of the biceps muscles at 1, 3, and 5 weeks postnatally ($P<0.05$).

Discussion

The purpose of the study was to compare the morphology and characteristics of motor endplates between the interossei muscles and the biceps muscles in Sprague-Dawley rats at 1, 3, and 5 weeks after birth. We found that there were more fragments of the motor endplate of the biceps muscles compared with that of the interossei muscles, and that the absolute area and the standard area of the motor endplate of the biceps muscles were both larger than those of the interossei muscles, and that after birth, the motor endplates of the interossei muscles and the biceps muscles gradually changed from crescent shape to pretzel shape.

The IMH include hypothenar muscles, interossei muscles, and lumbricals, whose functions are thumb opposition, and adduction, abduction, and stabilization of interphalangeal joints. They are mainly responsible for the fine regulation of finger joint activities. In contrast, the biceps muscles are responsible for gross movements such as the clasping reflex and elbow flexion (Schieber and Santello, 2004). It has been observed that there is an embrace reflex associated with large, rough movements of the biceps muscles after birth (Zafeiriou, 2004), while independent activities of palmar opposition of the thumb and individual fingers only occur at the age of 1 year, and the fine coordinated activities and development of each finger can be further improved by the age of 10 years (Schieber and Santello, 2004). The IMH are more specific in structure and function than any other skeletal muscle to ensure fine regulation. For instance, the interossei muscles have a relatively high cross-section area and a low fiber length/muscle length ratio, which make them capable of adapting to a high force output and low drift rate (Liss, 2012). In addition, the IMH of primates receive more corticospinal tract projections than the large muscles of the upper arms, and the IMH that dominate fine movements have a greater endplate/muscle fiber ratio than the powerful muscles (Gandevia and Kilbreath, 1990). Cranial muscles have a higher proportion of motor endplate area than limb muscles. In addition, laryngeal muscles have looser AChRs than limb muscles (Feng et al., 2012) and are less affected by muscle degenerative diseases (Marques et al., 2007; Thomas et al., 2008). Our study showed that, within 5 weeks after birth, the interossei muscles had a smaller motor endplate area and less morphological fragmentation than the biceps muscles. Therefore, there are differences in the development and maturity of the motor endplate between the IMH and the biceps muscles.

Surgical nerve reconstruction for denervated IMH after peripheral nerve injury produces modest results on average compared with denervated arm muscles. Approximately 5% of patients who undergo suturing of the ulnar nerve recover independent function of the IMH, while 77% of those who undergo repair of the musculocutaneous nerve achieve satisfying biceps tightening results (Jobe, 2008). In principle, the timing of nerve reconstruction operation should not exceed 9 months. However, the upper and middle trunk nerve reconstruction can be appropriately extended, and functional recovery can be obtained even after 30 months (Boome and Kaye, 1988). In contrast, the timing of the lower trunk nerve reconstruction should not exceed 6 months after birth; otherwise, the function of the interossei muscles cannot be improved (Chuang et al., 2005). To clarify the mechanism of earlier atrophy of the interossei muscles, our team found that miRNAs and mRNAs express differently in denervated IMF than in denervated biceps, and that most miRNAs and mRNAs are involved in the self-regulation of motor endplate in an OBPP rat model (Pan et al., 2015; Wu et al., 2016). In addition, inflammation and apoptosis play critical roles in aggravating atrophy of denervated IMF in a rat OBPP model at 3 and 5 weeks (Yu et al., 2020). In a rat OBPP

Table 1. Comparison of motor endplates between interossei and biceps muscles.

Parameters	Interossei muscles			Biceps muscles		
	1 week	3 weeks	5 weeks	1 week	3 weeks	5 weeks
Diameter of muscle fiber (μm)	11.2±0.7	19.4±2.4	21.9±1.3	14.7±0.9	21.3±1.3	26.9±2.03
Cross-sectional area of muscle fiber (μm^2)	137.3±23.3	176.7±43.2*	386.5±62.2*	139.9±18.4	253.0±35.8*	581.3±56.8*
Motor endplates area (μm^2)	78.3±10.0	145.0±9.1	197.5±16.2*	117.9±10.3	252.3±35.9	357.6±14.8*
[a]Normalized motor endplates area [a]($\mu m^2/\mu m$)	6.9±1.1*	7.6±0.9*	9.1±1.1*	8.0±0.9*	11.9±1.7*	13.4±1.0*

*$P<0.05$ (statistically significant difference between interossei and biceps muscles at 1, 3 and 5 weeks, respectively). [a]: Normalized motor endplate area: Divide the value of motor endplates area by its muscle fiber diameter.

model, downregulation of NRG-1/ErbB4 and phosphorylation of Akt/mTOR/p70S6K are associated with lower expression of AChR subunits. NRG-1/ErbB4 can enhance protein synthesis of the AChR subunits via phosphorylation of Akt/mTOR/p70S6K in L6 myoblasts (Qiao et al., 2022). In the same OBPP rat model, it was found that the degeneration of the motor endplate of the denervated IMF is more severe than that of the denervated biceps 5 weeks after denervation (Li et al., 2020). The ability to restore motor function in mice models of nerve transection/resuture can only be achieved by reinnervating motor synapse within five weeks of injury. After prolonged denervation, motor function cannot be recovered due to failure of motor endplate reformation rather than failure of axonal regeneration (Ma et al., 2011). Therefore, the difference in regulatory mechanism and reformation of the motor endplate maybe the most important factors affecting the morphology and distribution of motor endplates.

In this study, we found that the size of the motor endplates of the interossei muscles and the biceps muscles gradually increased at 1, 3, and 5 weeks after birth in SD rats. The metabolic stability of motor endplates increases after birth; the area and density of AChR clusters increase gradually; and the morphology changes from a "plaque" to a "pretzel" (Steinbach, 1981; Slater, 1982). This structural change helps to reduce the high resistance of the synaptic gap, thereby maintaining the high driving force of synaptic current. With the gradual maturation of synaptic wrinkles, AChRs gradually concentrate in the fold ridges (Fertuck and Salpeter, 1974). Synaptic regions are essential for maintaining muscle fiber action potentials. With the thickening of muscle fibers, the synaptic area becomes relatively small, and the amplitude of action potential decreases gradually. At this time, the depth and density of synaptic folds increase so as to increase the synaptic current and maintain the effectively transmitted action potential (Tapia et al., 2012). These studies indicate that the morphology and function of AChRs further differentiate and develop after birth, which is crucial for the effective transmission of action potential. Hence, the motor endplate undergoes a dynamic process of morphological maturation after birth.

The motor endplate changes within 2-3 weeks after birth. Embryonic AChRs are replaced by mature AChRs. The ε subunit of mature AChRs replaces the γ subunit to form the α2βεδ pentamer, which enables further condensing into high-density AChRs (Sakmann and Brenner, 1978; Matthews-Bellinger and Salpeter, 1983; Mishina et al., 1986; Jaramillo et al., 1988). During this period, the number of synaptic sites dominated by multiple neurons gradually decreases to a single axon (Redfern, 1970; Brown et al., 1976; Slater, 1982; Tapia et al., 2012). Within 2 weeks after birth, most of these motor neuron axons disappear, leaving only one axon for each muscle fiber. This process is called axonal withdrawal (Slater, 1982). In the process of axon withdrawal, axons projecting to the same synaptic site compete with each other, and the dominant axon occupies the synaptic site of the retreating axon (Walsh and Lichtman, 2003). It has been found that motor axon co-stimulation at the synaptic site can inhibit axon withdrawal in the model of transfer reinnervation (Busetto et al., 2000) and the model of in situ axon extrusion regeneration (Favero et al., 2010). When a denervated muscle is under dual control, if two neurons are stimulated at the same time, axon withdrawal will be inhibited (Favero et al., 2010). In contrast, asynchronous stimulation will promote axon withdrawal (Favero et al., 2012). The above studies suggest that axon withdrawal is regulated by electrical signals. Therefore, after birth, both the interossei muscles and the biceps muscles motor endplates undergo the change of AChRs from embryonic type to mature type and from multiple innervations to single innervation.

Our findings provide a model for studying the structural relationship between human brachial plexus injury and motor endplate, and also provide some useful information for the treatment of brachial plexus injury from the perspective of the motor endplate. For example, compared with the biceps muscles, the motor endplate of the interossei muscles is more prone to instability and degeneration. While trying to shorten the regeneration time from a donor nerve to receptor nerve, we can purposely delay the degeneration of the motor endplate, so as to gain time for nerve regeneration to reach the target organ and provide another way of thinking for providing clinical efficacy.

Conclusions

After birth, the morphology of the motor endplates of the interossei muscles and the biceps muscles gradually developed from the embryonic type to the mature type, and the appearance changed from a crescent to a pretzel shape. The interossei muscles showed a smaller motor endplate area and fewer fragments than the biceps muscles. A thorough study of the morphological differences between the motor endplates of the interossei muscles and the biceps muscles would be helpful to understand the pathological mechanism of irreversible atrophy of the IMF after peripheral nerve injury.

Ethical Publication statement. We confirm that we have read the journal's position on issues involved in ethical publication and affirm that this report is consistent with those guidelines.

Funding. The authors received no financial support for the research, authorship, and/or publication of this article.

Conflicts of Interests. The authors declare no potential conflicts of interest with respect to the research, authorship, and/or publication of this article.

References

Boome R.S. and Kaye J.C. (1988). Obstetric traction injuries of the

brachial plexus. Natural history, indications for surgical repair and results. J. Bone Joint Surg. Br. 70, 571-576.

Brown M.C., Jansen J.K. and Van Essen D. (1976). Polyneuronal innervation of skeletal muscle in new-born rats and its elimination during maturation. J. Physiol. (Lond.) 261, 387-422.

Busetto G., Buffelli M., Tognana E., Bellico F. and Cangiano A. (2000). Hebbian mechanisms revealed by electrical stimulation at developing rat neuromuscular junctions. J. Neurosci. 20, 685-695.

Chuang D.C., Mardini S. and Ma H.S. (2005). Surgical strategy for infant obstetrical brachial plexus palsy: experiences at Chang Gung Memorial Hospital. Plast. Reconstr. Surg. 116, 132-142.

Favero M., Buffelli M., Cangiano A. and Busetto G. (2010). The timing of impulse activity shapes the process of synaptic competition at the neuromuscular junction. Neuroscience 167, 343-353.

Favero M., Busetto G. and Cangiano A. (2012). Spike timing plays a key role in synapse elimination at the neuromuscular junction. Proc. Natl. Acad. Sci. USA 109, E1667-1675.

Feng X., Zhang T., Ralston E. and Ludlow C.L. (2012). Differences in neuromuscular junctions of laryngeal and limb muscles in rats. Laryngoscope 122, 1093-1098.

Fertuck H.C. and Salpeter M.M. (1974). Localization of acetylcholine receptor by 125I-labeled alpha-bungarotoxin binding at mouse motor endplates. Proc. Natl. Acad. Sci. USA 71, 1376-1378.

Gandevia S.C. and Kilbreath S.L. (1990). Accuracy of weight estimation for weights lifted by proximal and distal muscles of the human upper limb. J. Physiol. (Lond.) 423, 299-310.

Jaramillo F., Vicini S. and Schuetze S.M. (1988). Embryonic acetylcholine receptors guarantee spontaneous contractions in rat developing muscle. Nature 335, 66-68.

Jobe MT M.S.F. (2008). Peripheral nerve injuries. In: Campbell's Operative Orthopaedics. 11th ed. Canale S.T. and Beaty J.H. (eds). Mosby, Chicago. pp 3662-3687.

Kim Y.J., Brox T., Feiden W. and Weickert J. (2007). Fully automated segmentation and morphometrical analysis of muscle fiber images. Cytometry A 71, 8-15.

Li B., Chen L. and Gu Y.D. (2020). Stability of motor endplates is greater in the biceps than in the interossei in a rat model of obstetric brachial plexus palsy. Neural Regen. Res. 15, 1678-1685.

Lin J.S. and Samora J.B. (2022). Brachial plexus birth injuries. Orthop. Clin. North Am. 53, 167-177.

Liss F.E. (2012). The interosseous muscles: the foundation of hand function. Hand Clin. 28, 9-12.

Ma C.H., Omura T., Cobos E.J., Latrémolière A., Ghasemlou N., Brenner G.J., van Veen E., Barrett L., Sawada T., Gao F., Coppola G., Gertler F., Costigan M., Geschwind D. and Woolf C.J. (2011). Accelerating axonal growth promotes motor recovery after peripheral nerve injury in mice. J. Clin. Invest. 121, 4332-4347.

Marques M.J., Ferretti R., Vomero V.U., Minatel E. and Neto H.S. (2007). Intrinsic laryngeal muscles are spared from myonecrosis in the mdx mouse model of Duchenne muscular dystrophy. Muscle Nerve 35, 349-353.

Matthews-Bellinger J.A. and Salpeter M.M. (1983). Fine structural distribution of acetylcholine receptors at developing mouse neuromuscular junctions. J. Neurosci. 3, 644-657.

Mishina M., Takai T., Imoto K., Noda M., Takahashi T., Numa S., Methfessel C. and Sakmann B. (1986). Molecular distinction between fetal and adult forms of muscle acetylcholine receptor. Nature 321, 406-411.

Mukund K. and Subramaniam S. (2020). Skeletal muscle: A review of molecular structure and function, in health and disease. Wiley Interdiscip. Rev. Syst. Biol. Med. 12, e1462.

Pan F., Chen L., Ding F., Zhang J. and Gu Y.D. (2015). Expression profiles of MiRNAs for intrinsic musculature of the forepaw and biceps in the rat model simulating irreversible muscular atrophy of obstetric brachial plexus palsy. Gene 565, 268-274.

Pan F., Mi J.Y., Zhang Y., Pan X.Y. and Rui Y.J. (2016). Muscle fiber types composition and type identified endplate morphology of forepaw intrinsic muscles in the rat. J. Muscle Res. Cell. Motil. 37, 95-100.

Pfister J. and Zenker W. (1984). The splenius capitis muscle of the rat, architecture and histochemistry, afferent and efferent innervation as compared with that of the quadriceps muscle. Anat. Embryol. 169, 79-89.

Qiao J., Sun J., Chen L., Li B. and Gu Y. (2022). Neuregulin-1/ErbB4 upregulates acetylcholine receptors via Akt/mTOR/p70S6K: a study in a rat model of obstetric brachial plexus palsy and in vitro. Acta Biochim. Biophys. Sin. (Shanghai) 54, 1648-1657.

Redfern P.A. (1970). Neuromuscular transmission in new-born rats. J. Physiol. (Lond.) 209, 701-709.

Sakmann B. and Brenner H.R. (1978). Change in synaptic channel gating during neuromuscular development. Nature 276, 401-402.

Schieber M.H. and Santello M. (2004). Hand function: peripheral and central constraints on performance. J. Appl. Physiol. (1985) 96, 2293-2300.

Slater C.R. (1982). Postnatal maturation of nerve-muscle junctions in hindlimb muscles of the mouse. Dev. Biol. 94, 11-22.

Steinbach J.H. (1981). Developmental changes in acetylcholine receptor aggregates at rat skeletal neuromuscular junctions. Dev. Biol. 84, 267-276.

Tapia J.C., Wylie J.D., Kasthuri N., Hayworth K.J., Schalek R., Berger D.R., Guatimosim C., Seung H.S. and Lichtman J.W. (2012). Pervasive synaptic branch removal in the mammalian neuromuscular system at birth. Neuron 74, 816-829.

Thomas L.B., Joseph G.L., Adkins T.D., Andrade F.H. and Stemple J.C. (2008). Laryngeal muscles are spared in the dystrophin deficient mdx mouse. J. Speech Lang. Hear. Res. 51, 586-595.

Walsh M.K. and Lichtman J.W. (2003). *In vivo* time-lapse imaging of synaptic takeover associated with naturally occurring synapse elimination. Neuron 37, 67-73.

Wu J.X., Chen L., Ding F. and Gu Y.D. (2013). A rat model study of atrophy of denervated musculature of the hand being faster than that of denervated muscles of the arm. J. Muscle Res. Cell. Motil. 34, 15-22.

Wu J.X., Chen L., Ding F., Chen L.Z. and Gu Y.D. (2016). mRNA expression characteristics are different in irreversibly atrophic intrinsic muscles of the forepaw compared with reversibly atrophic biceps in a rat model of obstetric brachial plexus palsy (OBPP). J. Muscle Res. Cell. Motil. 37, 17-25.

Yu X.H., Wu J.X., Chen L. and Gu Y.D. (2020). Inflammation and apoptosis accelerate progression to irreversible atrophy in denervated intrinsic muscles of the hand compared with biceps: proteomic analysis of a rat model of obstetric brachial plexus palsy. Neural Regen. Res. 15, 1326-1332.

Zafeiriou D.I. (2004). Primitive reflexes and postural reactions in the neurodevelopmental examination. Pediatr. Neurol. 31, 1-8.

Accepted October 13, 2023